Nonlinear Functional Analysis and Applications
Vol. 29, No. 2 (2024), pp. 597-620
ISSN: 1229-1595(print), 2466-0973(online)

https://doi.org/10.22771/nfaa.2024.29.02.17
http://nfaa.kyungnam.ac.kr/journal-nfaa

IMPACT OF FRACTIONAL CONFORMABLE DERIVATIVES ON A(H1N1) INFECTION MODEL

Hind Ali Ahmad Eid[1] and Mohammed N Alkord[2]

[1]Najah National University
e-mail: h.eid@najah.edu

[2]Department of Mathematics, Mulana Azad Colleg reserch centre,
Dr.Babasaheb Ambekar Marthwada University, India
e-mail: moh1992alkord@gmail.com

Abstract. In this study, the conformable fractional derivative(CFD) of order ϱ in conjunction with the LC operator of orderρ is used to develop the model of the transmission of the A(H1N1) influenza infection. A brand-new A(H1N1) influenza infection model is presented, with a population split into four different compartments. Fixed point theorems were used to prove the existence of the solutions and uniqueness of this model. The basic reproduction number R_0 was determined. The least and most sensitive variables that could alter R_0 were then determined using normalized forward sensitivity indices. Through numerical simulations carried out with the aid of the Adams-Moulton approach, the study also investigated the effects of numerous biological characteristics on the system. The findings demonstrated that if $\varrho < 1$ and $\rho < 1$ under the CFD, also the findings demonstrated that if $\varrho = 1$ and $\rho = 1$ under the CFD, the A(H1N1) influenza infection will not vanish.

1. Introduction

Fractional calculus has become a basic tool for modeling phenomena involving memory. However, due to the non-local nature of fractional derivatives, the computations involved in solving fractional differential equations (FDEs) are tedious and time-consuming [11, 12]. Developing numerical and analytical

[0]Received October 23, 2023. Revised February 11, 2024. Accepted February 18, 2024.
[0]2020 Mathematics Subject Classification: 34B15, 34A08; 47H10.
[0]Keywords: A(H1N1) model, conformable derivative, fixed point theorem, Adams-Moulton approach.
[0]Corresponding author: Hind Ali Ahmad Eid (h.eid@najah.edu).

methods for solving nonlinear FDEs has been a subject of intense research at present [13]. Across the span of human history, infectious diseases have continuously threatened the general health of individuals, persistently standing as the primary cause of extensive suffering and mortality in developing nations. The spread of infectious diseases is influenced by various factors, such as the nature of the infectious agent, transmission routes, incubation and infectious periods, as well as the susceptibility and immunity of individuals. The agents responsible for infectious diseases demonstrate adaptability and possess adaptive characteristics, contributing to the emergence of novel infectious diseases and the resurgence of previously known ones. Illustrative instances of recently identified diseases include conditions like Lyme disease (discovered in 1975), Legionnaire's disease (1976), toxic shock syndrome (1978), hepatitis C (1989), hepatitis E (1990), and Hantavirus (1993). The virus (HIV) responsible for (AIDS) emerged in 1981 and has since become an important global sexually transmitted disease. In addition, strains of tuberculosis, pneumonia, and gonorrhea resistant to antibiotics have developed. Simultaneously, there has been a resurgence of illnesses such as malaria, dengue, and yellow fever, expanding their geographical range into previously untouched places, mostly due to changes in climatic patterns. Diseases like plague, cholera, and several hemorrhagic fevers, including but not limited to Bolivian, Ebola, Lassa, COVID-19, and Marburg, persistently manifest themselves intermittently [1, 4, 23].

The emergence of the H1N1 strain, implicated in the ongoing worldwide pandemic of swine-origin influenza, was first identified along the Mexico-United States border in April 2009. Within a short span of 2 months, it became the first pandemic of the 21st century [3].

H1N1 influenza known as swine flu is a subtype of influenza that may affect both people and animals [16, 24]. The virus is a zoonotic disease that may infect pigs, birds, horses, and other animals. Swine have been recognized as crucial influenza virus mixing vessels, enabling reassortment among diverse influenza virus strains due to their vulnerability to infection by both human and avian influenza viruses [2, 10]. The virus is named for the two proteins on its surface, hemagglutinin (H1) and neuraminidase (N1). Consequently, there are 18 H1 subtypes and 11 N1 subtypes, with H1N1 and H3N2 being endemic in humans [22]. H1N1 influenza is a respiratory virus with symptoms comparable to the common cold, including fever, cough, sore throat, runny or stuffy nose, muscular pains, and exhaustion [7, 16].

Before 2009, the identical triple-reassorted virus was discovered in pigs as early as 1998, with occasional human infections [18]. The H1N1 2009 virus (A/2009/H1N1) caused the first pandemic influenza of the new century, affecting over 214 regions and killing over 18,449 people [20].

In some cases, the H1N1 flu might result in more serious diseases, such as pneumonia, bronchitis, and even death [9]. The H1N1 virus is transmitted from person to person by droplets of air that form when a person with the virus breathes or sneezes. These tiny particles may enter the lips or noses of persons close to the infected person or be inhaled into the lungs [5].

Many mathematical models, consisting of fractional differential equations and fractional differential operators, have emerged to describe the H1N1 virus, control its spread, and understand its transmission mechanisms between people. For example, Shahram Rezapour et al. [21] explore the SEIR epidemic model, evaluate the stability of the disease-free equilibrium point, and research the influence of the derivative order on the actions of the resultant functions. Sina Etemad et al. [8] formulated a novel model of the A(H1N1)/09 influenza virus using advanced operators known as the fractalfractional operators, which have two fractal orders and fractional orders through power law-type kernels.

Khalil introduced a novel concept of the derivative called the "CFD" that seamlessly aligns with the classical derivative, exhibiting adherence to several standard properties, including the chain rule. Furthermore, it proves valuable in solving conformable differential equations. A CFD shares many characteristics with a classical derivative and has been used to model several physical and biological problems. The author used a mathematical operator called the conformable derivative (CD), in the sense of the Liouville-Caputo operator, to investigate measles infection [19].

In the current study, we investigate the SEIR epidemic model for the spread of A(H1N1) influenza under the CFD in the Liouville-Caputo sense. We first verify the existence and uniqueness of the model solution and then discuss the fundamental characteristics of the model, such as the disease-free equilibrium and basic reproduction number sensitivity. Additionally, the A(H1N1) model with the conformable-Liouville-Caputo operator is numerically solved using the Adams-Moulton technique, and the graphical effects of different parameters are shown for various values of the fractional order. This study aims to investigate the behavior of the A(H1N1) influenza model under different ϱ values and to analyze the effect of different factors on the disease dynamics. The primary contribution of this study is predicting the acutely infectious and chronically infectious courses at different derivative orders and studying the courses of the acutely infectious and chronically infectious at different values of the rate of contact between acutely infectious people and chronically infectious.

This research paper is presented as follows: In Sec 2, we offer some fundamental topics related to fractional calculus. We provide the model structure and its associated outcomes in Sec 3. In Sec 4, we will prove the existence

and uniqueness of results using the Liouville-Caputo operator. In Sec 5, we calculate disease-free equilibrium and R_0. The sensitivity analysis of the R_0 was discussed in Sec 6. Sec 7 shows an active numerical sketch for the H1N1 model solution by asymptomatic transporters.

2. Preliminaries

We give some definitions and their properties for our main results. Here are some fundamental ideas that will be used in this study.

Definition 2.1. [17] Let $\xi(t)$ is a differentiable and integrable function on R. Then for $t \in [r, b]$ and $\varrho > 0$,

(1)
$$^{RL}D^{\varrho}_{r,t}\xi(t) = \frac{1}{\Gamma(n-\varrho)}\frac{d^n}{dt^n}\int_r^t (t-s)^{n-\varrho-1}\xi(s)ds, \tag{2.1}$$
is the left Riemann-Liouville (RL) fractional derivative of order $\varrho > 0$,

(2)
$$^{RL}D^{\varrho}_{t,b}\xi(t) = \frac{1}{\Gamma(n-\varrho)}\frac{d^n}{dt^n}\int_t^b (s-t)^{n-\varrho-1}\xi(s)ds, \tag{2.2}$$
is the right (RL) fractional derivative of order $\varrho > 0$

where Γ is the gamma function.

Definition 2.2. [17] The Liouville–Caputo (LC) fractional derivative of non integer order ϱ may be expressed as follows:
$$^{LC}D^{\varrho}_{r,t}\xi(t) = \frac{1}{\Gamma(n-\varrho)}\int_r^t (t-s)^{n-\varrho-1}\frac{d^n}{ds^n}\xi(s)ds, \quad \varrho \in (n-1, n], \ \varrho > 0. \tag{2.3}$$

Definition 2.3. [15] The expression:
$$^{\rho}D^{\varrho}_{r,t}\xi(t) = \lim_{\tau\to 0}\frac{\xi(t+\tau t^{1-\varrho}) - \xi(t)}{\tau}, \tag{2.4}$$
where $\varrho, t > 0$, is called CFD of order ϱ.

The most crucial feature of CFD that links it with classical derivatives is as
$$^{rho}D^{\varrho}_{r,t}\xi(t) = (t-r)^{1-\varrho}\frac{d}{dt}\xi(t). \tag{2.5}$$

Definition 2.4. [15] Let $\xi(t) \in C^n_{r,b}([r, b]), Re(\rho) \geq 0$ and $n = \lceil \rho \rceil + 1$. Then the fractional conformable derivative with Caputo is defined as:
$$^{\rho}_{c}D^{\varrho}_{r,t}\xi(t) = ^{\rho}_{k} D^{\varrho}_{r,t}[\xi(t) - \sum_{k=0}^{n-1}\frac{^{\varrho}_{r}T_{r,t}\xi(r)}{k!\varrho^k}](t-r)^{\varrho k}](x). \tag{2.6}$$

Definition 2.5. [15] Let $\xi(t) \in C^n_{r,b}([r,b]), Re(\rho) \geq 0$ and $n = \lceil \rho \rceil + 1$. Then the fractional conformable derivative with Liouville-Caputo is defined as

$$\begin{aligned} {}^{\rho}_{c}D^{\varrho}_{r,t}\xi(t) &= \frac{1}{\Gamma(n-\rho)} \int_r^t (\frac{(t-r)^{\varrho} - (s-r)^{\varrho}}{\varrho})^{n-\rho-1} \frac{D^n_{r,t}}{(s-r)^{1-\varrho}} \xi(s) ds \\ &= c^{n-\rho} I^{\varrho}_{a,t} \xi(t) (c^n D^{\varrho}_{r,t} \xi(t)). \end{aligned} \tag{2.7}$$

Definition 2.6. [15] Let $\xi(t) \in C^n_{r,b}([r,b]), Re(\rho) \geq 0$ and $n = \lceil \rho \rceil + 1$. Then the fractional conformable integral in the sense of Liouville-Caputo is defined as

$${}^{\rho}\mathscr{I}^{\varrho}_{r,t}\xi(t) = \frac{1}{\Gamma(\rho)} \int_r^t (\frac{(t-r)^{\varrho} - (s-r)^{\varrho}}{\varrho})^{\rho-1} \frac{\xi(s)}{(s-r)^{1-\varrho}} ds. \tag{2.8}$$

Lemma 2.7. [15] *Let* $\xi(t) \in C^n_{r,b}([r,b]), Re(\rho) \geq 0$ *and* $n = \lceil \rho \rceil + 1$.

$${}^{\rho}_{r}\mathscr{I}^{\varrho}({}^{\rho}_{r}D^{\varrho}\xi(t)) = \xi(t) - \sum_{k=0}^{n-1} \frac{{}^{k}_{r}D^{\varrho}\xi(r)(t-r)^{\varrho k}}{\varrho^k \Gamma(k+1)}. \tag{2.9}$$

3. Formulation of the conformable A(H1N1) model

First, we will introduce the classical A(H1N1) model . The A(H1N1) model, which was presented in [21], divides the total population $\mathcal{N}(t)$ into four distinct subpopulations: susceptible individuals S, individuals incubating the virus E, infectious individuals I, and recovered individuals R. Furthermore, we denote to birth rate by τ, while individuals exit the system due to mortality at a rate denoted as ι. An individual in the class S migrates to the class E due to the transmission of the A(H1N1) virus by individuals in the class I, facilitated through effective interpersonal contacts occurring at a rate denoted by ν. In conclusion, it is important to note that upon an individual's recovery, they develop enduring immunity.

The additional parameters of the model include the recovery rate μ from the infection and the rate at which latent individuals become infected δ. The A(H1N1) model, which is scaled to the population size, is considered without any loss of generality and assumes a constant population size.

$$\begin{aligned}
\frac{dS}{dt} &= \tau\nu SI\iota S,\\
\frac{dE}{dt} &= \nu SI(\iota+\delta)E,\\
\frac{dE}{dt} &= \delta E(\iota+\mu)I,\\
\frac{dR}{dt} &= \mu I\iota R.
\end{aligned} \tag{3.1}$$

We will provide model (3.1) in a CFD of order ϱ with the LC operator of order ρ. We suggest the below H1N1 infectious model:

$$\begin{aligned}
{}^{\rho}D^{\varrho}_{0,t}S &= \tau\nu SI\iota S,\\
{}^{\rho}D^{\varrho}_{0,t}E &= \nu SI(\iota+\delta)E,\\
{}^{\rho}D^{\varrho}_{0,t}I &= \delta E(\iota+\mu)I,\\
{}^{\rho}D^{\varrho}_{0,t}R &= \mu I\iota\mathbb{R},
\end{aligned} \tag{3.2}$$

where $S(0)=S_0>0, E(0)=E_0>0, I(0)=I_0>0, \mathbb{R}(0)=\mathbb{R}_0\geq 0$ are initial conditions.

4. Existence and Uniqueness of Solution

The existence of the solution and its uniqueness with the non-integer conformable derivative order ϱ regarding the LC operator of order ρ will be demonstrated here for model (3.2).

Suppose the real-valued function $\mathbb{Z}(\mathbb{I})$ is continuous and contains the sup norm property as a Banach space on $\mathbb{I}=[0,b]$ and $P=\mathbb{Z}(\mathbb{I})\times\mathbb{Z}(\mathbb{I})\times\mathbb{Z}(\mathbb{I})\times\mathbb{Z}(\mathbb{I})$ with norm $\|(S,\ E,\ I,\ \mathbb{R})\|=\|S\|+\|E\|+\|I\|+\|\mathbb{R}\|,\ \|S\|=\sup_{t\in\mathbb{I}}|S|,\ \|E\|=\sup_{t\in\mathbb{I}}|E|,\ \|I\|=\sup_{t\in\mathbb{I}}|I|,\ \|\mathbb{R}\|=\sup_{t\in\mathbb{I}}|\mathbb{R}|$.

Using the fractional integral operator on both sides of model (3.2), we get

$$\begin{aligned}
S-S(0) &=^{\rho} \mathscr{I}^{\varrho}_{0,t}[\tau\nu SI\iota S],\\
E-E(0) &=^{\rho} \mathscr{I}^{\varrho}_{0,t}[\nu SI(\iota+\delta)E],\\
I-I(0) &=^{\rho} \mathscr{I}^{\varrho}_{0,t}[\delta E(\iota+\mu)I],\\
\mathbb{R}-\mathbb{R}(0) &=^{\rho} \mathscr{I}^{\varrho}_{0,t}[\mu I\iota\mathbb{R}],
\end{aligned} \tag{4.1}$$

by using Definition 2.5 which implies

$$S-S(0)=\frac{1}{\Gamma(\rho)}\int_r^t\Big(\frac{(t-r)^{\varrho}-(s-r)^{\varrho}}{\varrho}\Big)^{\rho-1}\frac{\xi_1(\rho,s,S(s))}{(s-r)^{1-\varrho}}ds,$$

$$
\begin{aligned}
E - E(0) &= \frac{1}{\Gamma(\rho)} \int_r^t \Big(\frac{(t-r)^{\varrho} - (s-r)^{\varrho}}{\varrho}\Big)^{\rho-1} \frac{\xi_2(\rho, s, E(s))}{(s-r)^{1-\varrho}} ds, \\
I - I(0) &= \frac{1}{\Gamma(\rho)} \int_r^t \Big(\frac{(t-r)^{\varrho} - (s-r)^{\varrho}}{\varrho}\Big)^{\rho-1} \frac{\xi_3(\rho, s, I(s))}{(s-r)^{1-\varrho}} ds, \\
\mathbb{R} - \mathbb{R}(0) &= \frac{1}{\Gamma(\rho)} \int_r^t \Big(\frac{(t-r)^{\varrho} - (s-r)^{\varrho}}{\varrho}\Big)^{\rho-1} \frac{\xi_4(\rho, s, \mathbb{R}(s))}{(s-r)^{1-\varrho}} ds,
\end{aligned} \tag{4.2}
$$

where

$$
\begin{aligned}
\xi_1(\rho, t, S) &= \tau \nu S I \iota S, \\
\xi_2(\rho, t, E) &= \nu S I (\iota + \delta) E, \\
\xi_3(\rho, t, I) &= \delta E (\iota + \mu) I, \\
\xi_4(\rho, t, \mathbb{R}) &= \mu I \iota \mathbb{R}.
\end{aligned} \tag{4.3}
$$

The symbols ξ_1, ξ_2, ξ_3, and ξ_4 have to hold for the Lipschitz condition only if S, E, I, and $\mathbb{R}$ possess an upper bound. Suppose that S and S^* are couple functions, we have

$$
\begin{aligned}
\|\xi_1(\rho, t, S) - \xi_1(\rho, t, S^*)\| &= \|\tau \nu S I \iota S - (\tau - \nu S^* I - \iota S^*)\|, \\
\|\xi_1(\rho, t, E) - \xi_1(\rho, t, E^*)\| &= \|\nu S I (\iota + \delta) E - (\nu S I - (\iota + \delta) E^*)\|, \\
\|\xi_1(\rho, t, I) - \xi_1(\rho, t, I^*)\| &= \|\delta E (\iota + \mu) I - (\delta E - (\iota + \mu) I^*)\|, \\
\|\xi_1(\rho, t, \mathbb{R}) - \xi_1(\rho, t, \mathbb{R}^*)\| &= \|\mu I m \mathbb{R} - (\mu I - \iota \mathbb{R}^*)\|.
\end{aligned} \tag{4.4}
$$

Now by taking ω_1 as

$$
\begin{aligned}
\omega_1 &= \|\nu I + \iota\|, \\
\omega_2 &= \|\iota + \delta\|, \\
\omega_3 &= \|\iota + \mu\|, \\
\omega_4 &= \|\iota\|.
\end{aligned} \tag{4.5}
$$

Iontinuing in the same manner above, we get

$$
\begin{aligned}
\|\xi_1(\rho, t, S) - \xi_1(\rho, t, S^*)\| &\leq \omega_1 \|S - S^*\|, \\
\|\xi_1(\rho, t, E) - \xi_1(\rho, t, E^*)\| &\leq \omega_2 \|E - E^*\|, \\
\|\xi_1(\rho, t, I) - \xi_1(\rho, t, I^*)\| &\leq \omega_3 \|I - I^*\|, \\
\|\xi_1(\rho, t, \mathbb{R}) - \xi_1(\rho, t, \mathbb{R}^*)\| &\leq \omega_4 \|\mathbb{R} - \mathbb{R}^*\|.
\end{aligned} \tag{4.6}
$$

This means that the Lipschitz condition has been done for all four functions.

Now let us take the expressions in an iterative way. Indeed, (4.2) yields

$$\begin{aligned}
S_n - S(0) &= \frac{1}{\Gamma(\rho)}\int_r^t (\frac{(t-r)^\varrho - (s-r)^\varrho}{\varrho})^{\rho-1}\frac{\xi_1(\rho,s,S_{n-1}(s))}{(s-r)^{1-\varrho}}ds,\\
E_n - E(0) &= \frac{1}{\Gamma(\rho)}\int_r^t (\frac{(t-r)^\varrho - (s-r)^\varrho}{\varrho})^{\rho-1}\frac{\xi_2(\rho,s,E_{n-1}(s))}{(s-r)^{1-\varrho}}ds,\\
I_n - I(0) &= \frac{1}{\Gamma(\rho)}\int_r^t (\frac{(t-r)^\varrho - (s-r)^\varrho}{\varrho})^{\rho-1}\frac{\xi_3(\rho,s,I_{n-1}(s))}{(s-r)^{1-\varrho}}ds,\\
\mathbb{R}_n - \mathbb{R}(0) &= \frac{1}{\Gamma(\rho)}\int_r^t (\frac{(t-r)^\varrho - (s-r)^\varrho}{\varrho})^{\rho-1}\frac{\xi_4(\rho,s,\mathbb{R}_{n-1}(s))}{(s-r)^{1-\varrho}}ds,
\end{aligned} \tag{4.7}$$

with $S(0) = N_1, E(0) = N_2, I(0) = N_3, \mathbb{R}(0) = N_4$.

When the difference between the following terms is taken, we obtain

$$\begin{aligned}
\Upsilon_{S,n} &= S_n - S_{n-1}\\
&= \frac{1}{\Gamma(\rho)}\int_r^t (\frac{(t-r)^\varrho - (s-r)^\varrho}{\varrho})^{\rho-1}\frac{(\xi_1(\rho,s,S_{n-1}(s)) - \xi_1(\rho,s,S_{n-2}(s)))}{(s-r)^{1-\varrho}}ds,
\end{aligned}$$

$$\begin{aligned}
\Upsilon_{E,n} &= E_n - E_{n-1}\\
&= \frac{1}{\Gamma(\rho)}\int_r^t (\frac{(t-r)^\varrho - (s-r)^\varrho}{\varrho})^{\rho-1}\frac{(\xi_2(\rho,s,E_{n-1}(s)) - \xi_2(\rho,s,E_{n-2}(s)))}{(s-r)^{1-\varrho}}ds,
\end{aligned}$$

$$\begin{aligned}
\Upsilon_{I,n} &= I_n - I_{n-1}\\
&= \frac{1}{\Gamma(\rho)}\int_r^t (\frac{(t-r)^\varrho - (s-r)^\varrho}{\varrho})^{\rho-1}\frac{(\xi_3(\rho,s,I_{n-1}(s)) - \xi_3(\rho,s,I_{n-2}(s)))}{(s-r)^{1-\varrho}}ds,
\end{aligned} \tag{4.8}$$

$$\begin{aligned}
\Upsilon_{\mathbb{R},n} &= \mathbb{R}_n - \mathbb{R}_{n-1}(0)\\
&= \frac{1}{\Gamma(\rho)}\int_r^t (\frac{(t-r)^\varrho - (s-r)^\varrho}{\varrho})^{\rho-1}\frac{(\xi_4(\rho,s,\mathbb{R}_{n-1}(s)) - \xi_4(\rho,s,\mathbb{R}_{n-2}(s)))}{(s-r)^{1-\varrho}}ds.
\end{aligned}$$

It is important to note that, $S_n = \sum_{i=1}^{n}\Upsilon_{S,i},\ E_n = \sum_{i=1}^{n}\Upsilon_{E,i},\ I_n = \sum_{i=1}^{n}\Upsilon_{I,i}$, and $\mathbb{R}_n = \sum_{i=1}^{n}\Upsilon_{\mathbb{R},i}$. As well, by using (4.6), (4.7), (4.8) and fact that $\Upsilon_{S,n-1} = S_{n-1} - S_{n-2}$, $\Upsilon_{E,n-1} = E_{n-1} - E_{n-2}$, $\Upsilon_{I,n-1} = I_{n-1} - I_{n-2}$, $\Upsilon_{\mathbb{R},n-1} = \mathbb{R}_{n-1} -$

$\mathbb{R}_{n-1}$, we have

$$\begin{aligned}
\|\Upsilon_{S,n}\| &\leq \frac{1}{\Gamma(\rho)}\omega_1 \int_r^t (\frac{(t-r)^{\varrho}-(s-r)^{\varrho}}{\varrho})^{\rho-1} \frac{\|\Upsilon_{S,n-1}\|}{(s-r)^{1-\varrho}} ds,\\
\|\Upsilon_{E,n}\| &\leq \frac{1}{\Gamma(\rho)}\omega_2 \int_r^t (\frac{(t-r)^{\varrho}-(s-r)^{\varrho}}{\varrho})^{\rho-1} \frac{\|\Upsilon_{E,n-1}\|}{(s-r)^{1-\varrho}} ds,\\
\|\Upsilon_{I,n}\| &\leq \frac{1}{\Gamma(\rho)}\omega_3 \int_r^t (\frac{(t-r)^{\varrho}-(s-r)^{\varrho}}{\varrho})^{\rho-1} \frac{\|\Upsilon_{I,n-1}\|}{(s-r)^{1-\varrho}} ds,\\
\|\Upsilon_{\mathbb{R},n}\| &\leq \frac{1}{\Gamma(\rho)}\omega_4 \int_r^t (\frac{(t-r)^{\varrho}-(s-r)^{\varrho}}{\varrho})^{\rho-1} \frac{\|\Upsilon_{\mathbb{R},n-1}\|}{(s-r)^{1-\varrho}} ds.
\end{aligned} \tag{4.9}$$

Now, the next theorem shall be proven.

Theorem 4.1. *Suppose that*

$$\frac{1}{\Gamma(\rho+1)}\omega_j < 1,\ \ i = 1,2,3,4. \tag{4.10}$$

Then model (3.2) has a unique solution for $t \in [0,b]$.

Proof. It is clear that functions S, E, I and $\mathbb{R}$ are bounded. Additionally, from (4.5) and (4.6), the symbols ξ_1, ξ_2, ξ_3 and ξ_4 are satisfy the Lipchitz condition. Taking (4.9) along with a recursive hypothesis, we get

$$\begin{aligned}
\|\Upsilon_{S,n}\| &\leq \|S_0\|(\frac{1}{\Gamma(\rho+1)}\omega_1)^n,\\
\|\Upsilon_{E,n}\| &\leq \|E_0\|(\frac{1}{\Gamma(\rho+1)}\omega_2)^n,\\
\|\Upsilon_{I,n}\| &\leq \|I_0\|(\frac{1}{\Gamma(\rho+1)}\omega_3)^n,\\
\|\Upsilon_{\mathbb{R},n}\| &\leq \|\mathbb{R}_0\|(\frac{1}{\Gamma(\rho+1)}\omega_4)^n.
\end{aligned} \tag{4.11}$$

As a result, it is evident that $\|\Upsilon_{S,n}\| \longrightarrow 0, \|\Upsilon_{A,n}\| \longrightarrow 0, \|\Upsilon_{I,n}\| \longrightarrow 0$, and $\|\Upsilon_{\mathbb{R},n}\| \longrightarrow 0\, as\, n \longrightarrow \infty$. Moreover, from (4.11) and imposing the triangle,

we obtain

$$\begin{aligned}
\|S_{n+k} - S_n\| &\leq \sum_{j=n+1}^{n+k} r_1^j = \frac{r_1^{n+1} - r_1^{n+k+1}}{1 - r_1}, \\
\|E_{n+k} - E_n\| &\leq \sum_{j=n+1}^{n+k} r_2^j = \frac{r_2^{n+1} - r_2^{n+k+1}}{1 - r_2}, \\
\|I_{n+k} - I_n\| &\leq \sum_{j=n+1}^{n+k} r_3^j = \frac{r_3^{n+1} - r_3^{n+k+1}}{1 - r_3}, \\
\|\mathbb{R}_{n+k} - \mathbb{R}_n\| &\leq \sum_{j=n+1}^{n+k} r_4^j = \frac{r_4^{n+1} - r_4^{n+k+1}}{1 - r_4},
\end{aligned} \tag{4.12}$$

with $r_i := \frac{1}{\Gamma(\rho+1)}\omega_i < 1$, by (4.10). Thus, S_n, E_n, I_n and $\mathbb{R}_n$ are Cauchy sequences in the Banach space $Z(\mathbb{I})$.

This proves that it is uniformly convergent [6]. The limit of (4.7) as $n \longrightarrow \infty$ confirms unique solution of these sequences and satisfy the model (3.2). This ensures that existence of a unique solution for model (3.2) in according to (4.10). □

5. Disease-free equilibrium (DFE)

To calculate the equilibrium point of the model (3.2), we make the model's left side (3.2) equal to zero as follows:

$$\begin{aligned}
&\tau\nu SI\iota S = 0, \\
&\nu SI(\iota + \delta)E = 0, \\
&\delta E(\iota + \mu)I = 0, \\
&\mu I\iota\mathbb{R} = 0.
\end{aligned} \tag{5.1}$$

By solving the algebraic equations, we obtain equilibrium points of system (3.2). The disease free equilibrium point is obtained as

$$E_0 = (S, E, I, \mathbb{R}) = (\frac{\tau}{\iota}, 0, 0, 0).$$

Theorem 5.1. *The DFE E_0 ought to achieve $Re(\xi_j) < 0,\ j = 1, \ldots, 4$ for being locally asymptotically stable (LAS), when ξ the eigenvalue of the Jacobian matrix calculated at such free equilibrium .*

Proof. Since the linearization method is used, the DFE point $J(E_0)$ its LAS can be checked. So, the Jacobian matrix is denoted by $J(E_0)$:

$$\begin{bmatrix} -\iota & 0 & -\nu\frac{\tau}{\iota} & 0 \\ 0 & -(\iota+\delta) & \nu\frac{\tau}{\iota} & 0 \\ 0 & \delta & -(\iota+\mu) & 0 \\ 0 & 0 & \mu & -\iota \end{bmatrix}. \tag{5.2}$$

It is not difficult to get eigenvalues of the above 4×4 Jacobian matrix, We obtained two different eigenvalues, and another one repeated twice, as given below:

$$-\iota < 0\ , -(\iota+\delta) < 0,\ -(\iota+\mu) < 0 \tag{5.3}$$

Since all of the parameters are positive,then the eigenvalues of the above 4×4 Jacobian matrix are negative, So the E_0 of the disease is (LAS). □

5.1. **Basic reproduction number** (R_0)**.** R_0 is the number of infected cases due to the transmission of infection from a previously injured person. It can be calculated as explained by Van den Driessche in [25]. By using the relation $R_0 = \lambda(FV^{-1})$, where λ the spectral radius of the second generation operator, F and V are the matrices for the new disease class and for the rest of transitional terms, respectively. The matrices F and V connected to model (3.2) are given by:

$$f = \begin{bmatrix} \nu SI \\ 0 \end{bmatrix}. \tag{5.4}$$

$$v = \begin{bmatrix} (\iota+\delta)E \\ -\delta E + (\iota+\mu)] \end{bmatrix}, \tag{5.5}$$

$$F = \begin{bmatrix} 0 & \nu S_0 \\ 0 & 0 \end{bmatrix}. \tag{5.6}$$

Since $S_0 = \frac{\tau}{\iota}$, then

$$F = \begin{bmatrix} 0 & \nu\frac{\tau}{\iota} \\ 0 & 0 \end{bmatrix} \tag{5.7}$$

and

$$V = \begin{bmatrix} (\iota+\delta) & 0 \\ \delta & (\iota+\mu) \end{bmatrix}, \tag{5.8}$$

$$V^{-1} = \begin{bmatrix} \frac{1}{(\iota+\delta)} & 0 \\ \frac{\delta}{(\iota+\delta)(\iota+\mu)} & \frac{1}{(\iota+\mu)} \end{bmatrix}. \tag{5.9}$$

So

$$FV^{-1} = \begin{bmatrix} \frac{\tau\delta\nu}{\iota(\iota+\delta)(\iota+\mu)} & \frac{\tau\nu}{\iota(\iota+\mu)} \\ 0 & 0 \end{bmatrix}. \tag{5.10}$$

The expression for R_0 is the spectral radius of the matrix FV^{-1} and is written as follows $R_0 = \frac{\nu\delta\tau}{\iota(\iota+\delta)(\iota+\mu)}$, which is less than one, by using [26], we can say that the DFE point is locally stable and that the population cannot be infected by the illness.

6. Analysis of the fundamental reproduction number's sensitivity

In this portion, we explain a sensitivity analysis performed on a subset of the parameters in the proposed model (3.2). As a result, it will be easier to distinguish between factors in terms of their positive or negative effect on the basic reproduction rate. We find it by using method given in [26] and using $R_0 = \frac{\nu\delta\tau}{\iota(\iota+\delta)(\iota+\mu)}$, as:

$$\begin{aligned} \propto_{\tau}^{R_0} &= \frac{\partial R_0}{\partial \tau}\frac{\tau}{R_0} = 1, \quad \propto_{\nu}^{R_0} = 1, \quad \propto_{\mu}^{R_0} = \frac{-\mu}{\mu+\iota} < 0, \\ \propto_{\iota}^{R_0} &= -1 - \frac{\iota}{\iota+\delta} - \frac{\iota}{\mu+\iota} < 0, \quad \propto_{\delta}^{R_0} = \frac{\iota}{(\iota+\delta)} < 1. \end{aligned} \tag{6.1}$$

Table 1. Description of the parameters of the model (3.2).

Parameters	Sensitivity indices
τ	1
ν	1
δ	0.0014977
μ	-0.9987
ι	-0.0027977

Through the Table 1, the sensitivity indices ν, τ and δ are greater than zero and μ and ι, are not. thus R_0 is decreasing with τ and δ while rising with ν, τ and δ.

7. Discussion and numerical results

In this part, we discuss the numerical simulations for the A(H1N1) infectious model (3.2) with the aid of an iterative method known as the Adams-Moulton technique, Hoofnagle [14] used approximate solutions of fractional type of (ODE) to get different results of emulations for state variables $(S,\ E,\ I,\ \mathbb{R})$

contained in the H1N1 infectious model (3.2). The Cauchy ODE by the LC operator of the order ρ has been considered as the following:

$$\begin{aligned} &{}_c^{\rho}D_{0,t}y(t) = f(t, y(t)),\ \rho > 0,\ t \in [0, B], \\ &y^{(j)}(0) = y_{(0)}^{(j)}, \end{aligned} \tag{7.1}$$

where$j = 0, 1, 2, \ldots, \lceil \rho \rceil - 1$. The Cauchy-mentioned above initial value problem can be turned into a Volterra integral equation of the second kind as follows:

$$y(t) = \Sigma_{j=0}^{n-1} y_{(0)}^{(j)} \frac{t^j}{j!} + \frac{1}{\Gamma(\rho)} \int_0^t (t-\zeta)^{\rho-1} f(\zeta, y(\zeta)) d\zeta \quad , \rho \in (n-1, n]. \tag{7.2}$$

To get the repeated approach, we suppose the constant time step size $\triangle t = \frac{B}{N},\ t_j = j \triangle t,\ \ j = 0, 1, 2, \ldots, N$ where N is the number of times of integration in the interval $[0, B]$. Estimating the preceding equation in terms of fractions by taking the differential operator into account the of order ϱ, we get the Adams Moulton technique [19] for the CFD of order ϱ with LC operator of order ρ:

$$y_{n+1} = y(0) + \frac{(\triangle t)^{\rho}}{b\Gamma(\rho)} \Sigma_{j=0}^{n} [(n+1-j)^{\rho} - (n-j)^{\rho}] D_{0,t}^{\varrho} f(t_j, y_j), j \in [0, n]. \tag{7.3}$$

By using the CFD of order ϱ then we get:

$$D_{0,t}^{\varrho} f(t_j, y(t_j)) = \frac{1}{t_j^{\varrho-1}} \frac{d}{dt} f(t_j, y(t_j)), \varrho > 0. \tag{7.4}$$

Now, by applying the iterative process described in (7.3), the H1N1 model (3.2) with the CFD of order ϱ with (LC) operator of order ρ can be expressed as follows:

$$\begin{aligned} S_{n+1} &= S(0) + \frac{(\triangle t)^{\rho}}{\rho\Gamma(\rho)} \Sigma_{j=0}^{n} [(n+1-j)^{\rho} - (n-j)^{\rho}] D_{0,t}^{\varrho} f_1(t_j, S_j, E_j, I_j, \mathbb{R}_j), \\ E_{n+1} &= E(0) + \frac{(\triangle t)^{\rho}}{\rho\Gamma(\rho)} \Sigma_{j=0}^{n} [(n+1-j)^{\rho} - (n-j)^{\rho}] D_{0,t}^{\varrho} f_2(t_j, S_j, E_j, I_j, \mathbb{R}_j), \\ I_{n+1} &= I(0) + \frac{(\triangle t)^{\rho}}{\rho\Gamma(\rho)} \Sigma_{j=0}^{n} [(n+1-j)^{\rho} - (n-j)^{\rho}] D_{0,t}^{\varrho} f_3(t_j, S_j, E_j, I_j, \mathbb{R}_j), \\ \mathbb{R}_{n+1} &= \mathbb{R}(0) + \frac{(\triangle t)^{\rho}}{\rho\Gamma(\rho)} \Sigma_{j=0}^{n} [(n+1-j)^{\rho} - (n-j)^{\rho}] D_{0,t}^{\varrho} f_4(t_j, S_j, E_j, I_j, \mathbb{R}_j), \end{aligned} \tag{7.5}$$

where

$$f_1(t_j, S_j, E_j, I_j, \mathbb{R}_j) = \frac{1}{t_j^{\varrho-1}}[\tau\nu SI\iota S],$$
$$f_2(t_j, S_j, E_j, I_j, \mathbb{R}_j) = \frac{1}{t_j^{\varrho-1}}[\nu SI(\iota+\delta)E],$$
$$f_3(t_j, S_j, A_j, I_j, \mathbb{R}_j) = \frac{1}{t_j^{\varrho-1}}[\delta E(\iota+\mu)I],$$
$$f_4(t_j, S_j, A_j, I_j, \mathbb{R}_j) = \frac{1}{t_j^{\varrho-1}}[\mu I\iota\mathbb{R}],$$

Throughout simulations, Δt is the magnitude of the time step is equal 10^{-1}. The interval time is $[0, 100]$ and it is arbitrarily supposed that the initial conditions $(0.999,\ 0,\ 0.001,\ 0)$, also the biological parameters are chosen to be $\tau = 0.0003, \iota = 0.0003,\ \nu = 2.5,\ \mu = 0.14,\ \delta = 0.2,\ \rho = 0.94,\ \varrho$ value chosen to be $(0.8,\ 0.85,\ 0.90,\ 0.95$ and $1)$.

Our simulations are based on continuous model tracking, where the order of derivative and parameters are considered for different values.

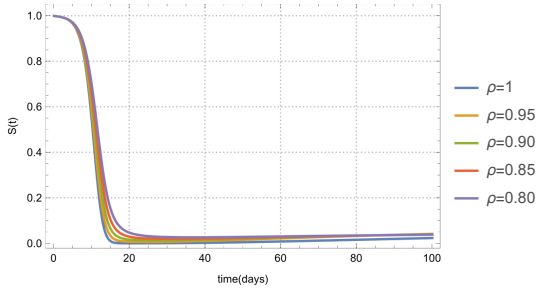

FIGURE 1. The approximate solution of S of the considered model (3.2) for ρ value chosen to be $(0.8,\ 0.85,\ 0.90,\ 0.95$ and $1)$.

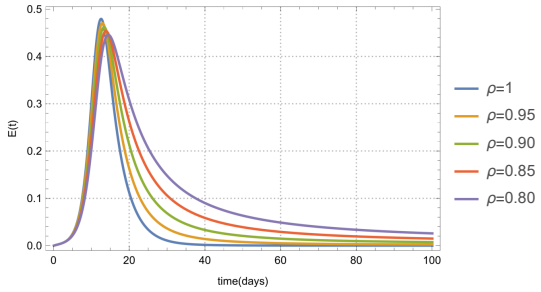

FIGURE 2. The approximate solution of E of the considered model (3.2) for ρ value chosen to be $(0.8,\ 0.85,\ 0.90,\ 0.95$ and $1)$.

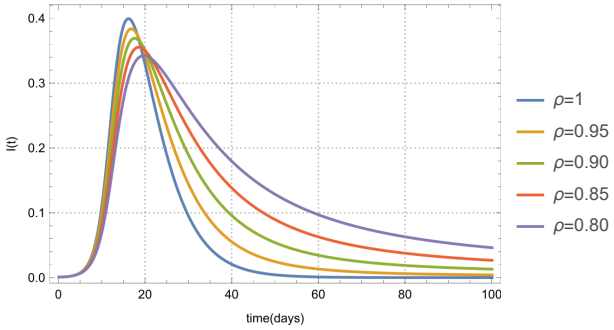

FIGURE 3. The approximate solution of I of the considered model (3.2) for ρ value chosen to be (0.8, 0.85, 0.90, 0.95 and 1).

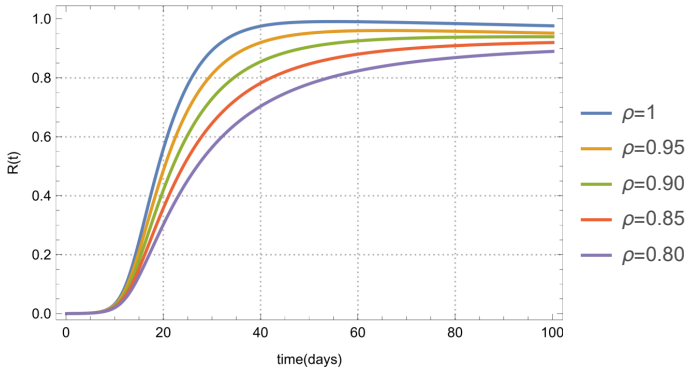

FIGURE 4. The approximate solution of $\mathbb{R}$ of the considered model (3.2) for ρ value chosen to be (0.8, 0.85, 0.90, 0.95 and 1).

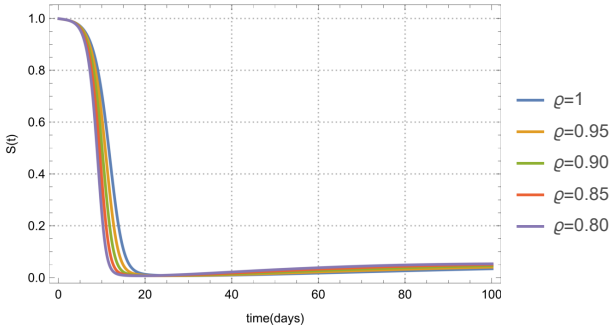

FIGURE 5. The approximate solution of S of the considered model (3.2) for different values of ϱ.

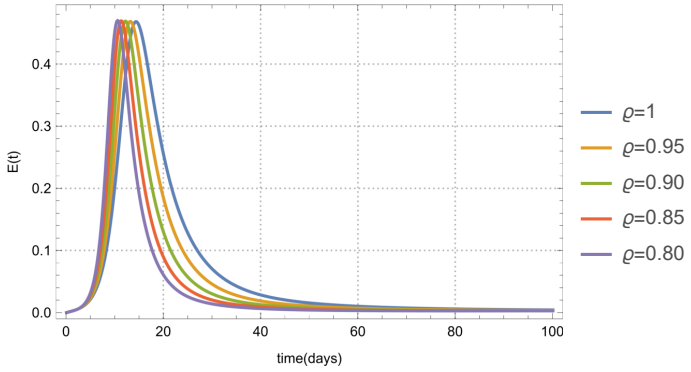

FIGURE 6. The approximate solution of E of the considered model (3.2) for different values of ϱ.

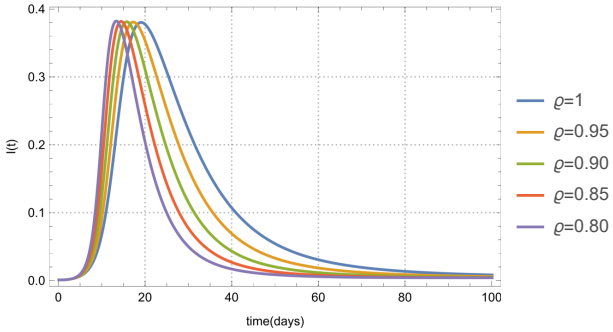

FIGURE 7. The approximate solution of I of the considered model (3.2) for different values of ϱ.

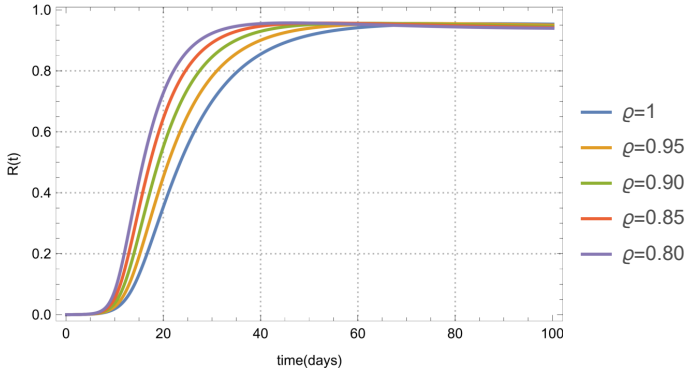

FIGURE 8. The approximate solution of $\mathbb{R}$ of the considered model (3.2) for different values of ϱ.

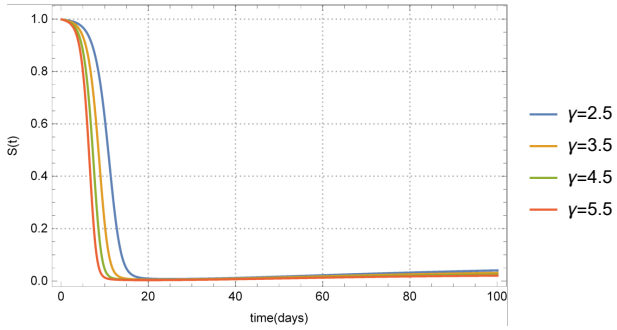

FIGURE 9. The approximate solution of S of the considered model (3.2) varying the value of λ and using a fixed value for $\varrho = 0.95$ and $\rho = 0.94$.

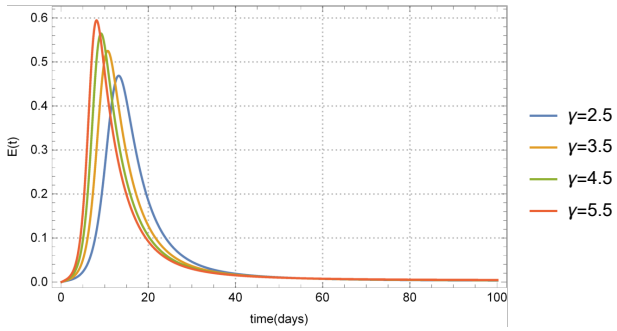

FIGURE 10. The approximate solution of E of the considered model (3.2) varying the value of λ and using a fixed value for $\varrho = 0.95$ and $\rho = 0.94$.

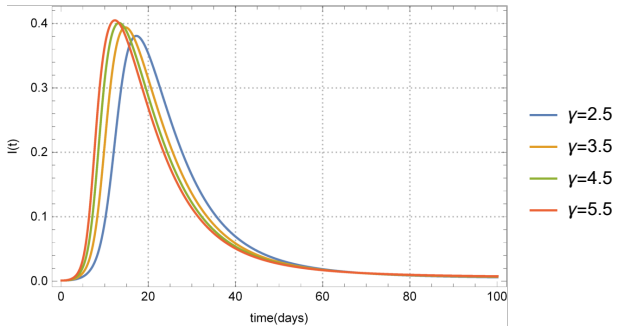

FIGURE 11. The approximate solution of I of the considered model (3.2)varying the value of λ and using a fixed value for $\varrho = 0.95$ and $\rho = 0.94$.

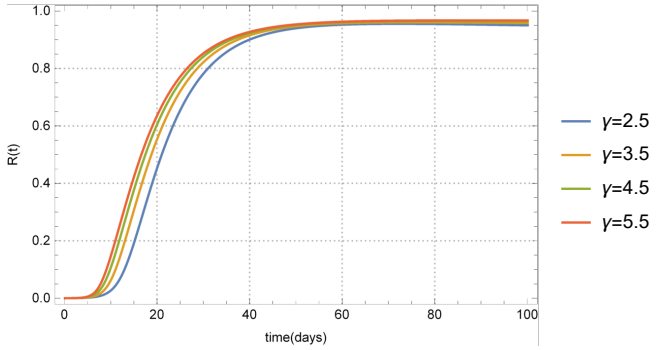

FIGURE 12. The approximate solution of $\mathbb{R}$ of the considered model (3.2) varying the value of λ and using a fixed value for $\varrho = 0.95$ and $\rho = 0.94$.

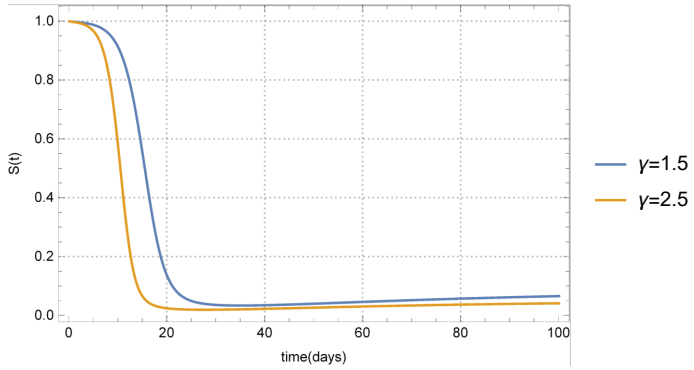

FIGURE 13. clearfy susceptible population S at order $\varrho = 0.90$, $\rho = 0,85$ while other parameters are as mentioned above.

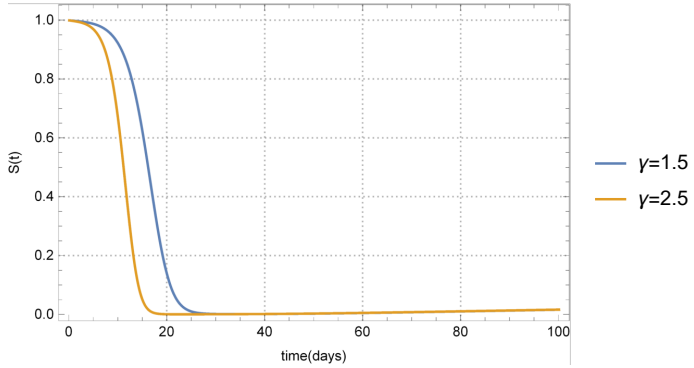

FIGURE 14. clearfy susceptible population S at order $\varrho = 1$, $\rho = 1$ while other parameters are as mentioned above.

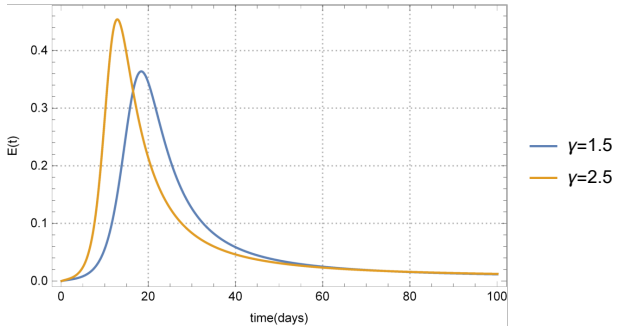

FIGURE 15. clearfy class E at order $\varrho = 0.90$, $\rho = 0.85$ while other parameters are as mentioned above.

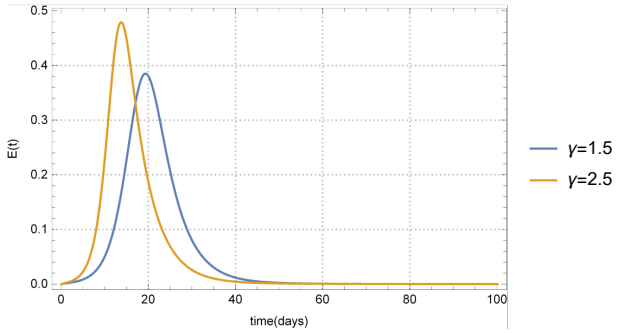

FIGURE 16. clearfy E at order $\varrho = 1$, $\rho = 1$ while other parameters are as mentioned above.

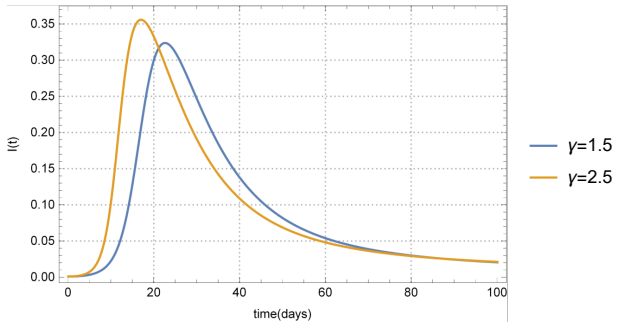

FIGURE 17. clearfy I with mentioned operator of order $\varrho = 0.90$, $\rho = 0.85$ while other parameters are as mentioned above.

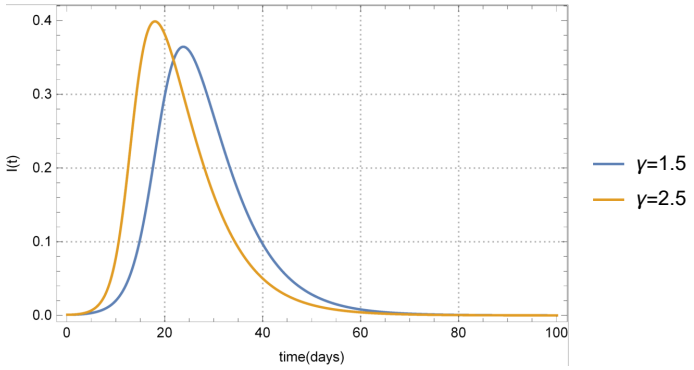

FIGURE 18. clearfy I with mentioned operator of order $\varrho = 1$, $\rho = 1$ while other parameters are as mentioned above.

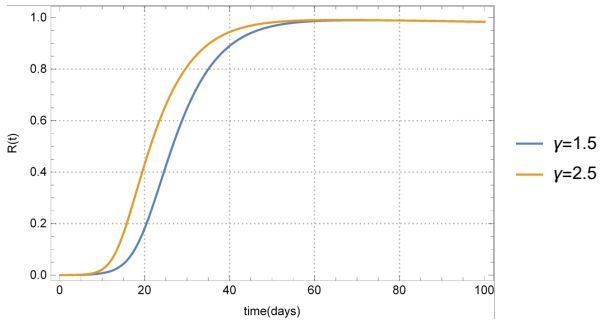

FIGURE 19. clearfy $\mathbb{R}$ with mentioned operator of order $\varrho = 1$, $\rho = 1$ while other parameters are as mentioned above.

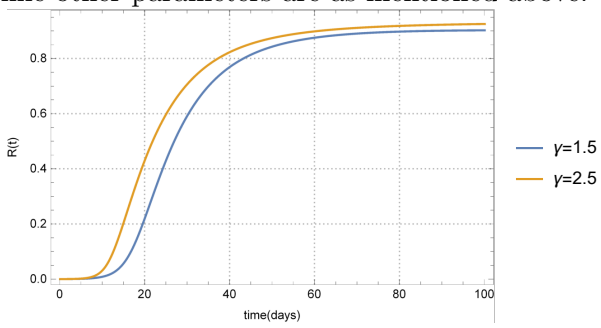

FIGURE 20. clearfy $\mathbb{R}$ with mentioned operator of order $\varrho = 0.90$, $\rho = 0.85$ while other parameters are as mentioned above.

The approximate solution of the mathematical model is illustrated in fig. 1 figs. 2 to 4 for various values of ρ, while keeping $\varrho = 0.95$ constant. In the fig. 5, a decrease in the representation curve for the susceptible population is observed due to an increase in the infection transmission rate from the infected group, leading to a rise in the number of infected individuals, as depicted in fig. 6, and fig. 7, during the initial fifteen days.

Additionally, mild recovery cases are noted during this period. However, after the first 20 days, an increase in recovery processes is witnessed, as shown in fig. 8. We also simulated the model for different values of ϱ , as in fig. 5, fig. 6, fig. 7, fig. 8. In fig. 9, fig. 10, fig. 11, fig. 12,we altered the transmission rate from an infectious class to another and assigned values to ϱ and ρ as 0.95 and 0.94, respectively. It was found that an increase in the infection transmission rate leads to more infections and a shortened virus incubation period, and vice versa. In the fig. 13 and fig. 14, we assigned values to γ the values (1.5 and 2.5) and compared the fractional model with $\varrho = 0.90$ and $\rho = 0.85$, to the proper-order model with $\varrho = 1$ and $\rho = 1$. Notably fig. 13, for $\gamma = 1.5$ infections do not spread to the entire exposed group, leaving a few unaffected after 25 days.

Comparisons were also made for the categories (E, I, $\mathbb{R}$) in fig. 15, fig. 16, fig. 17, fig. 18, fig. 20 and fig. 19. It is observed from figs. 1 to 4 that the increase and decrease in the values of $E, I, \mathbb{R}$ are proportional to the changes in ρ, while the variations in ϱ, result in constant increases and decreases, as seen in figs. 5 to 8. We found that the model with the fractional order is more representative and accurate than the model with integer order.

Conclusion

In this study, the CFD of order ϱ in conjunction with the Liouville-Caputo operator of order ρ is used to develop the model of the transmission of the A H1N1 influenza infection. A brand-new A(H1N1) influenza infection model is presented, with a population split into four different compartments. Fixed point theorems were used to investigate the existence of the solutions and uniqueness of this model. The system's basic reproduction number R_0 was determined. The least and most sensitive variables that could alter R_0 were then determined using normalized forward sensitivity indices. Through numerical simulations carried out with the aid of the Adams-Moulton approach, the study also investigated the effects of numerous biological characteristics on the system. The findings demonstrated that if $\varrho < 1$ and $\rho < 1$ under the CFD, also the findings demonstrated that if $\varrho = 1$ and $\rho = 1$ under the CFD, the A(H1N1) influenza infection will not vanish.

In our forthcoming research endeavors, we aim to enhance the model by incorporating more intricate dynamics, such as demographics, waning immunity, and vaccination. We plan to estimate model parameters by aligning them with real epidemiological data, ensuring a more accurate representation of the underlying dynamics.

Our future work also involves the development of optimal control strategies to effectively curb infection spread and reduce the basic reproduction number.This entails a comprehensive examination of the model's parameters and their impact on disease dynamics.

Furthermore, we intend to conduct a thorough dynamical systems analysis, including the creation of bifurcation diagrams, to explore qualitative changes in the model's dynamics. This analysis will provide valuable insights into the system's behavior under various conditions.

To broaden the scope of our research, we propose extending the model to accommodate multiple strains, allowing for an in-depth investigation into strain interaction and competition. Additionally, we plan to create a metapopulation version, incorporating spatial dynamics to study interconnected subpopulations.

In our comparative analysis, we will assess the model under various fractional derivative definitions, such as Caputo-Fabrizio and Atangana-Baleanu, to evaluate their impact on the model's behavior.

To ensure the practical relevance of our model, we will validate its predictions against empirical data and refine the model based on observed mismatches. This iterative validation process will enhance the model's reliability and predictive accuracy.

References

[1] P. Agarwal, M. A. Ramadan, A. M. Rageh, and A. R. Hadhoud, *A fractional-order mathematical model for analyzing the pandemic trend of COVID-19,* Math. Meth. Appl. Sci., **45**(8) (2022), 4625–4642.

[2] S. Bangaru, K. Thamotharan, S. Manickam, A. K. Ramasamy, and R. Perumalsamy, *Probing the Ononin and Corylin molecules against anti-influenza H1N1 A virus: a detailed active site analysis,* Res. Chemical Intermed., **2023** (2023), 1–20.

[3] L.-Y. Chang, S.-R. Shih, P.-L. Shao, D. T.-N. Huang, and L.-M. Huang, *Novel swine-origin influenza virus A (H1N1): the first pandemic of the 21st century,* J. Formosan Medical Ass., **108**(7) (2009), 526–532.

[4] Y. Chen, F. Liu, Q. Yu, and T. Li, *Review of fractional epidemic models,* Appl.Math. Mod., **97** (2021), 281–307.

[5] G. Chowell, S. M. Bertozzi, M. A. Colchero, H. Lopez-Gatell, C. Alpuche-Aranda, M. Hernandez, and M. A. Miller, *Severe respiratory disease concurrent with the circulation of H1N1 influenza,* New England J. Medicine, **361**(7) (2009), 674–679.

[6] K. Diethelm, N. J. Ford, and A. D. Freed, *A predictor-corrector approach for the numerical solution of fractional differential equations,* Nonlinear Dyna., **29** (2002), 3–22.
[7] F. P. Esper, T. Spahlinger, and L. Zhou, *Rate and influence of respiratory virus co-infection on pandemic (H1N1) influenza disease,* J. Infection, **63**(4) (2011), 260–266.
[8] S. Etemad, I. Avci, P. Kumar, D. Baleanu, and S. Rezapour, *Some novel mathematical analysis on the fractal–fractional model of the AH1N1/09 virus and its generalized Caputo-type version,* Chaos, Solitons & Fractals, **162** (2022), 112511.
[9] G. González-Parra, A. J. Arenas, and B. M. Chen-Charpentier, *A fractional order epidemic model for the simulation of outbreaks of influenza A (H1N1),* Math. Meth. Appl. Sci., **37**(15) (2014), 2218–2226.
[10] J. S. Griffith and L. E. Orgel, *Ligand-field theory,* Quarterly Rev. Chem. Soc., **11**(4) (1957), 381–393.
[11] A. R. Hadhoud, A. M. Rageh, and T. Radwan, *Computational solution of the time-fractional Schrödinger equation by using trigonometric B-spline collocation method,* Fractal and Fractional, **6**(3) (2022), 127.
[12] A. R. Hadhoud, H. M. Srivastava, and A. M. Rageh, *Non-polynomial B-spline and shifted Jacobi spectral collocation techniques to solve time-fractional nonlinear coupled Burgers equations numerically,* Adv. Diff. Equ., **2021** (2021), 1–28.
[13] A. R. Hadhoud, P. Agarwal, and A. M. Rageh, *Numerical treatments of the nonlinear coupled time-fractional Schrödinger equations,* Math. Meth. Appl. Sci. **45**(11) (2022), 7119–7143.
[14] J. H. Hoofnagle, *Chronic type B hepatitis,* Gastroenterology, **84**(2) (1983), 422–424.
[15] F. Jarad, E. Uğurlu, T. Abdeljawad, and D. Baleanu, *On a new class of fractional operators,* Adv. Diff. Equ., **2017**(1) (2017), 1–16.
[16] B. H. Lim and T. A. Mahmood, *Influenza A H1N1 2009 (swine flu) and pregnancy,* The J. Obstetrics and Gynecology of India, **61** (2011), 386–393.
[17] K. S. Miller and B. Ross, *An introduction to the fractional calculus and fractional differential equations,* Wiley, 1993.
[18] C. W. Olsen, *The emergence of novel swine influenza viruses in North America,* Virus Research, **85**(2) (2002), 199–210.
[19] S. Qureshi, *Effects of vaccination on measles dynamics under fractional conformable derivative with Liouville–Caputo operator,* The Euro. Phy.. J. Plus, **135**(1) (2020), 63.
[20] S. Rewar, D. Mirdha, and P. Rewar, *Treatment and prevention of pandemic H1N1 influenza,* Ann. Global Health, **81**(5) (2015), 645–653.
[21] S. Rezapour and H. Mohammadi, *A study on the AH1N1/09 influenza transmission model with the fractional Caputo–Fabrizio derivative,* Adv. Diff. Equ., **2020**(1) (2020), 1–15.
[22] A. Sakudo, K. Baba, M. Tsukamoto, A. Sugimoto, T. Okada, T. Kobayashi, N. Kawashita, T. Takagi, and K. Ikuta, *Anionic polymer, poly (methyl vinyl ether–maleic anhydride)-coated beads-based capture of human influenza A and B virus,* Bioorganic & Medicinal Chemistry, **17**(2) (2009), 752–757.
[23] E. Y. Salah, B. Sontakke, M. S. Abdo, W. Shatanawi, K. Abodayeh, M. D. Albalwi, and others, *Conformable Fractional-Order Modeling and Analysis of HIV/AIDS Transmission Dynamics,* Int. J. Diff. Equ., **2024** (2024).
[24] D. J. Sencer and J. D. Millar, *Reflections on the 1976 swine flu vaccination program,* Emerging Infectious Diseases, **12**(1) (2006), 29.
[25] P. Van den Driessche and J. Watmough, *Reproduction numbers and sub-threshold endemic equilibria for compartmental models of disease transmission,* Math. Biosciences, **180**(1-2) (2002), 29–48.

[26] M. Yavuz, F. Özköse, M. Susam, and M. Kalidass, *A new modeling of fractional-order and sensitivity analysis for hepatitis-b disease with real data,* Fractal and Fractional, **7**(2) (2023), 165.